Available online at www.sciencedirect.com

ScienceDirect

Procedia Manufacturing 41 (2019) 66–73

Procedia MANUFACTURING

www.elsevier.com/locate/procedia

8th Manufacturing Engineering Society International Conference, MESIC 2019, 19-21 June 2019, Madrid, Spain

Analysis of microstructure and defects in 17-4 PH stainless steel sample manufactured by Selective Laser Melting

Paola Leo [a]*, Sonia D'Ostuni [a], Patrizia Perulli [b], Maria Angeles Castro Sastre[c], Ana Isabel Fernández-Abia [c], Joaquin Barreiro [c]

[a] *University of Salento, Engineering Innovation Department, Via per arnesano s.n, Lecce 73100, Università del Salento. Italy*
[b] *Politecnico di Bari, DMMM - Department of Mechanics, Mathematics and Management, viale Japigia, 182 - Bari, Italy*
[c] *Dept. of Mechanical, Informatic and Aerospatiale Engineering. Universidad de León. Spain*

Abstract

The microstructure and defectiveness of a 17-4 PH sample produced by Selective Laser Melting using nitrogen atomized powder have been studied. The analysis has been performed in both longitudinal and transversal sections with regard to the printing direction. A very fine-grained microstructure has been revealed. The X-Ray analysis has shown the occurrence of both martensitic/ferritic α phase and austenitic ϒ phase. No significant differences in average hardness values have been observed for cross and longitudinal sections. The average hardness value in the bottom cross section has been found equal to 308±13 HV1/15. Some voids associated with inclusions and not fused powder have been observed. EDX analysis has been used to analyse the chemistry of the inclusions. The area fraction of defectiveness does not exceed the 1% and diameter of inclusions is generally lower than 20 µm.

Keywords: Selective Laser melting; microstructure; defectiveness; hardness; additive manufacturing.

* Corresponding author. Tel.: +39-0832-297324; fax: +39-0832-297324.
E-mail address: paola.leo@unisalento.it

© 2019 The Authors. Published by Elsevier B.V.
This is an open access article under the CC BY-NC-ND license (http://creativecommons.org/licenses/by-nc-nd/4.0/)
Peer-review under responsibility of the scientific committee of the 8th Manufacturing Engineering Society International Conference.

1. Introduction

Additive Manufacturing (AM) processes build three-dimensional (3D) parts by progressively adding very thin layers of materials guided by a digital model. Alloy powders are commonly used as feedstock materials in the laser beam assisted AM techniques due to ease of feeding and controlled melting [1].

Selective laser melting (SLM) is one of the powder bed fusion (PBF) processes, which are the most widely used in the AM industry. SLM is regarded as the most versatile AM process, because it can process a wide spectrum of materials, including Al-based alloys, Ti-based alloys, Ni-based alloys, Co-based alloys, Cu-based alloys, and Fe-based alloys [2]. Particularly, 17-4 PH alloy is a martensitic precipitation hardened (PH) stainless steel characterized by resistance to corrosion up to 300 °C and tailorable strengthening by copper precipitates. 17-4 PH is widely used as structural material in marine environments, power plants and chemical industries [3]. The excellent weldability of 17-4 PH stainless steel and its ability to be heat treated to improve mechanical properties make it a good material choice for SLM.

Qualities of additively manufactured parts are significantly influenced by occurrence of voids having a deleterious effect on the mechanical properties. In general terms, voids within PBF AM parts can be classified by their characteristic morphology. Porosity caused by entrapped gas is spherical and it can be influenced by powder packing density and powder manufacturing process. Porosity characterized by irregular shape is due to thermal stresses, incomplete melting of particles and balling effect caused by instability of the melt pool [1,4].The incomplete melting of the powder layer into the layer below leads to interlayer cracking and it causes elongated voids along the melt pool boundaries (lack of fusion porosity) [4].

The microstructure evolution induced by AM processes affects the properties of the component. Using high density processes (Laser Beam or Electron Beam), a higher cooling rate is induced in the melting pool, favoring a very fine microstructure and a significant metastability. Such a metastability may give rise to mechanical properties largely different from those of the as-cast and wrought materials. For example, 17-4 PH stainless steel component produced by Selective Laser melting (SLM) contains, after cooling, a high amount of metastable untransformed austenite because of the very fine microstructure [5]. That austenite can evolve into martensite only after a destabilization heat treatment [5]. The microstructure evolution is also a function of process parameters and gas environment (both for powder processing and building camera) [3].

2. Experimental set up

The 3D sample is a gear with a geometry shown in Fig.1a. Its height and external diameter are equal to 14 mm, the inner diameter is equal to 5 mm. This geometry was chosen to analyze the defects in a functional part with a relatively complex geometry and fine details. The sample was manufactured by a ProX 100 SLM machine located in “3D Printing and Manufacturing Unit” (UFI3D) at the University of León. This machine is equipped with a fiber laser under inert nitrogen atmosphere. The composition of the 17-4 PH alloy is shown in Table 1. Fig.1b shows the morphology of the nitrogen atomized powder obtained by Scanning Electron Microscope (ZEISS EVO Microscope). The average radius of the particles is equal to 6 ± 6 μm and the average shape factor (*f*circle) of the particles (equal to 1 for a perfect sphere) is equal to 0.87±0.09. So, the particles are mainly spherical (Fig.1b). The test sample was built according the process parameter listed in Table 2.

The microstructure of the sample was characterized along longitudinal and cross section surfaces, in top and bottom external surfaces. Optical microscope (OM) and scanning electron microscope (SEM) were used. Particularly, NIKON EPHIPHOT 200 optical Microscope and ZEISS EVO SEM Microscope equipped with a Bruker energy-dispersive X-Ray spectrometer (EDX) were used. The sections were prepared following the standard procedure. The microstructure was revealed using Kalling’s n.1 etching (1.5g $CuCl_2$, 33ml ethanol, 33ml water, 33 ml HCl). This etching provides a good contrast between martensite/ferrite (darker) and austenite (white, not attacked).

X Ray diffraction analysis (XRD) was performed on the specimen section perpendicular to the building direction. A Rigaku D/MAX-Ultima X-Ray system was employed for this analysis. Cu (Kα) X-radiation was used.

\

HV hardness was measured using a Vickers Affri Wiky 200JS digital instrument employing a 1 Kgf load and a 15 s dwell time. The hardness was measured in the same cross and longitudinal surfaces observed by OM.

By using NIS-Element (a NIKON software supplied with Epiphot 200 OM), the area fraction of defects was evaluated. Defects area percentage was measured as the sum of the defect areas divided by the area of the surfaces in the sample. Moreover, using ImageJ software, the defects Feret's diameter was evaluated.

Table 1. Chemical composition (Wt %) of the 17-4 PH alloy.

Element	Si	Cr	Ni	Cu	Fe
Wt (%)	0.62	16.93	4.17	3.56	74.72

Table 2. Process parameters.

Laser Power	50 W
Laser Speed	140 mm/s
Beam width	0.07 mm
Layer thickness	0.03 mm
Hatch style	concentric
Radius	5 mm
Overlap	50 µm
Post Build parameter	Air cooling

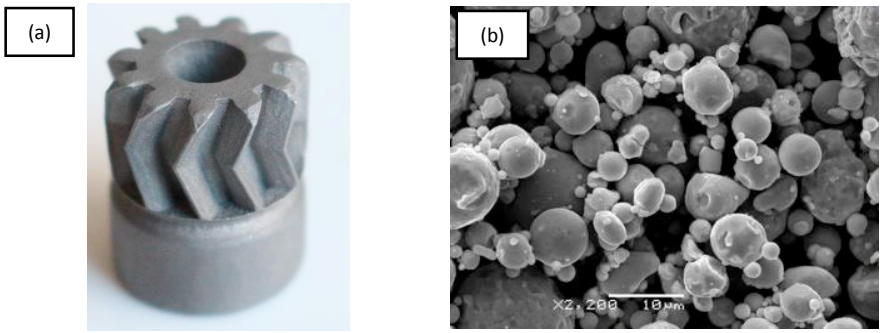

Fig. 1. (a) picture of the sample as received; (b) SEM micrograph of the nitrogen atomized powder.

3. Result and discussion

3.1. Microstructure and microhardness

The top and bottom surfaces and the longitudinal section of the sample were reconstructed as puzzles of optical micrographs at magnification equal to 50X, as reported in Fig.2a-c.

Higher magnification micrographs of both top and longitudinal surface after etching are shown in Fig.3 a,b. The cross section plane in Fig.3a is characterized by footprints of laser track visible as parallel lines. In the longitudinal plane (Fig.3b) the microstructure is characterized by bowl-like cross sections of the melt pools. The melt pool depth

exhibits some variation in size along the bowl like cross section, probably due to local instabilities. Due to the etching, both darker and lighter zones can be observed in Fig.3, often mixed together.

The XRD pattern for the top transverse plane (Fig.4a) shows the presence of both martensitic or ferritic α phase and austenitic ϒ phase. In fact, because of the very low carbon concentration in this alloy (0.035 wt%), the magnitude of the lattice distortion in the body-centered tetragonal (BCT) martensite is very small and it is not possible to distinguish between the body centered cubic (BCC) ferrite and the BCT martensite [6]. As such, with the used techniques, the sample microstructure could contain both ferritic/martensitic microstructure (usually observed in the 17-4 PH stainless steel) together with retained austenite. SEM micrograph of the top cross section plane in Fig.4b highlights the fine dendritic scale of the columnar grains together with the difference in dendritic morphology (elongated or equiaxed) and the occurrence of the different phases, sometime intimately mixed.

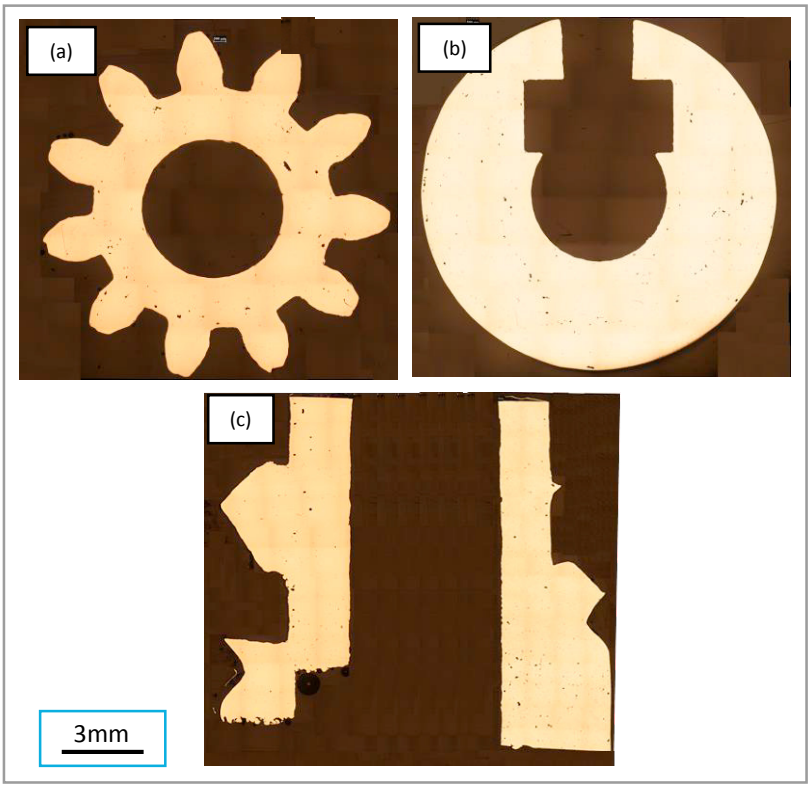

Fig. 2. Puzzle of optical micrographs at 50X (a) the top surface; (b) the bottom surface; (c) the longitudinal surface.

Conventionally, 17-4 PH exhibits a martensitic structure with a small fraction of ferrite. Unlike the traditional cast processes, the microstructure of the sample characterized in this study exhibit also austenitic phase. The observed austenitic microstructure depends on the high density energy process that favors a significant metastability [3, 5-8]. Moreover, even the type of gas used for both SLM and/or powder process affects the as-built microstructure. For example, Rafi et al [8] observed a higher portion of retained austenite in the as-built 17-4 PH sample when nitrogen atomized powder was processed under a nitrogen SLM atmosphere rather than argon atmosphere. Later, Meredith et al [9] have shown that, the atomization in nitrogen plays a prominent role respect to the gas used during the building process in promoting high level of retained austenite. Finally, even the austenitic grain refinement induced by the high cooling rate involved in SLM process leads to reduce the martensite start and so to increase the amount of retained austenite [10].

\

Microhardness measurements were performed on the longitudinal section along the sample height and along the diameter of both transversal surfaces. The average values of hardness coming from 8 measurements on each section are shown in Table 3. No significant variation of average values was detected for the different sections. The high values of standard deviation can be due to the occurrence of defectiveness and to the mixed microstructures.

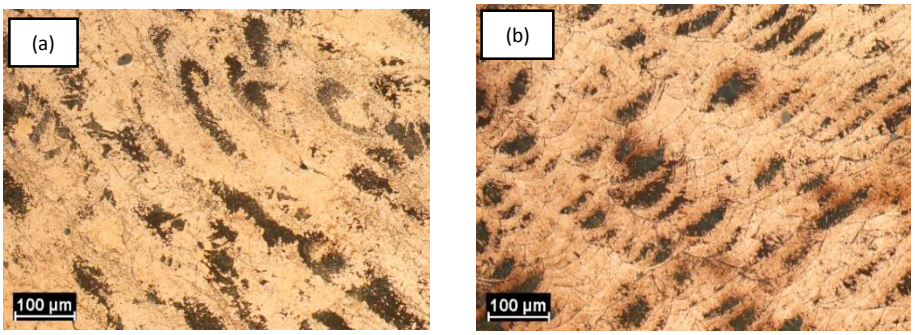

Fig. 3. Optical micrographs at 200X (a) the top surface; (b) the longitudinal section.

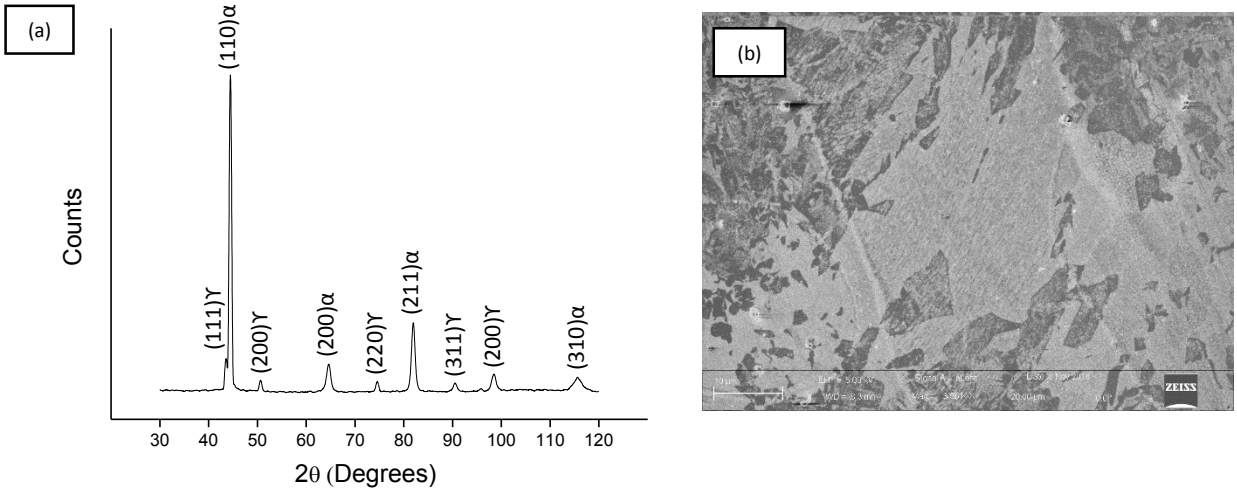

Fig. 4. (a) XRD pattern; (b) SEM micrograph of the top cross plane, confirming the presence of mixed phases and showing the fine scale and different morphology of the dendritic microstructure.

Table 3. Average hardness values.

Sections	Hardness [HV 1/15]
Upper surface	307.75 ± 13.3
Bottom surface	308.30 ± 13.0
Longitudinal surface	315.40 ± 10.0

3.2. Defects

All the surfaces shown in Fig.3 are characterized by defects with irregular morphology, as shown in more detail in Fig.5. These defects include inclusions and/or not fused powder as shown by the EDX spectra in Fig.5 c and are usually associated with voids. The area fraction of defectiveness was determined by image analysis on the three surfaces and it is listed in Table 4. The highest value was found in the longitudinal surface (0.52%). The distribution of the percentage of defectiveness with respect the diameter (Fig.6 a, b, c) indicates a high occurrence of defects with average diameter lower than 20 μm.

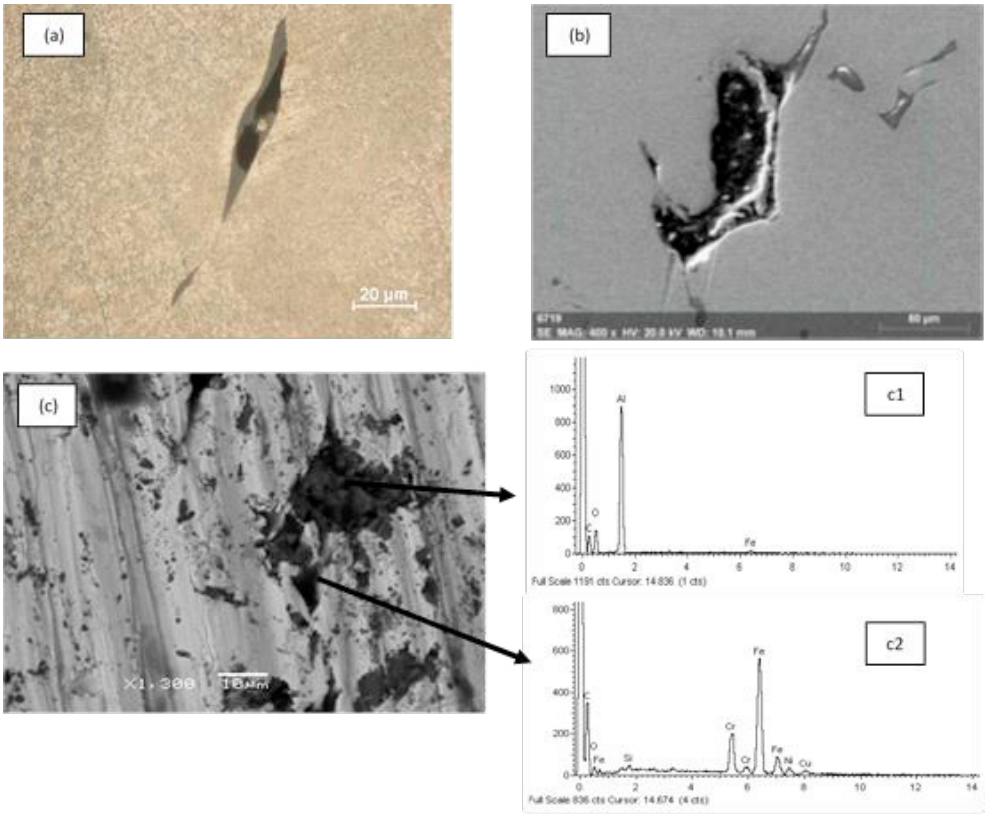

Fig. 5. (a) Optical micrograph of defectiveness in the sample; (b) SEM micrograph of defectiveness in the sample; (c) The defects include both voids and oxide inclusion or not fused area as result from EDS spectra close to voids occurrence: aluminum oxide (c1 spectrum) and non-fused particles (c2 spectrum).

Defectiveness appears preferentially along the melt pool boundaries and they are elongated in shape (Fig.5 a, b). According to EDX spectrum in Fig.5-c1, both oxygen and aluminum inclusions have been detected in the samples. Since Al is not present in the standard chemistry for 17-4 PH, the Al content that results from the spectrum in Fig.5-c1 is a strong indication that there was oxide contamination in the powder. In fact, during the standard gas atomization process, the alloy chemistry changes if the molten alloy touches ceramic components. If contaminants appears in the powder (for example oxide material from crucible), those contaminants will occur in the built SLM sample as shown by Y. Sun et al [11]. Moreover, the spectrum in Fig. 5-c2 shows the occurrence of not fused powder. Not fused powder is usually associated with lack of fusion or voids caused by inadequate penetration of the molten pool of an upper layer into the previously deposited layer [12, 13]. Inadequate penetration causes in the final product defects usually larger than 10 μm in equivalent diameter [14, 15].

\

Table 4. Summary of defects characterization.

Analyzed Surfaces	Surfaces area [mm^2]	Total defects area [mm^2]	Voids area fraction [%]
Top surface	81.20	0.28	0.34
Bottom surface	120.52	0.48	0.40
Longitudinal surface	73.15	0.38	0.52

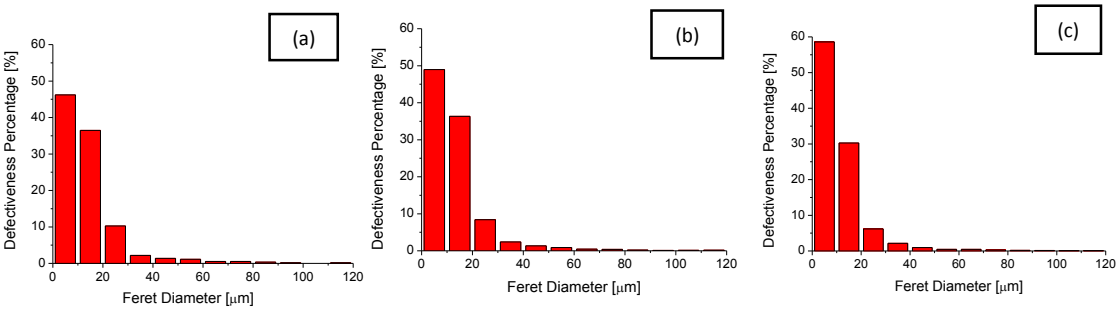

Fig. 6. Diameter distribution of defectiveness (a) the top surface; (b) the bottom surface; (c) the longitudinal section.

4. Conclusions

The following main conclusions can be drawn from this research:

1) The sample microstructure is mixed and fine grained. Unlike the traditional microstructure for 17-4 PH sample containing Ferrite and Martensite, the SLM microstructure of the sample characterized in this study exhibits also the austenitic phase.
2) The average Vickers hardness does not change significantly along all the analyzed surfaces. The average values are close to 310 HV in agreement with the mixed microstructure.
3) Defects of different size and diameter occurs in the sample. The defects include voids associated with aluminum oxide or not fused powder. These defects are irregular in shape and more than 80% have an average diameter lower than 20 μm. The area fraction of the defects is lower than 0.52%.

These valuable information is very important for optimizing the AM SLM process, by choosing adequately the operation parameters. Future works include the study of the influence of operation parameters in the microstructure and defects of the sample, in order to improve the final quality and properties of the parts. Also, the results of this research can be useful for AM powder manufacturers, so that they can optimize the powder atomization process taking into account the repercussion in the manufactured part by SLM.

Acknowledgements

Authors thank to Ministry of Science, Innovation and Universities of Spain for the support through the research project with reference DPI2017-89840-R and to the Junta de Castilla y León through the research project with reference FEDER P17-LE027P17.

References

[1] T. Debroy, H.L. Wei, J.S. Zuback , T. Mukherjee , J.W. Elmer , J.O. Milewski , A.M. Beese , A. Wilson-Heid A. De, W. Zhang, Additive manufacturing of metallic components – Process, structure and properties, Materials Science and Engineering, Materials Research Institute, 92 (2018) 112–224.

[2] P. K. Gokuldoss, S. Kolla, J. Eckert, Additive Manufacturing Processes: Selective Laser Melting, Electron Beam Melting and Binder Jetting—Selection Guidelines, Materials, 10,672 (2017) doi:10.3390/ma10060672.

[3] L. E. Murr, E. Martinez, J. Hernandez, S. Collins, K. N. Amato, S. M. Gaytan, P. W. Shindo, Microstructures and Properties of 17-4 PH Stainless Steel Fabricated by Selective Laser Melting, Journal of Materials Research Technology, 1-3 (2012) 167-177.

[4] A. Kudzal, B. McWilliams, C. Hofmeister, F. Kellogg, J. Yuc, J. Taggart-Scarff , J. Liang, Effect of scan pattern on the microstructure and mechanical properties of Powder Bed Fusion additive manufactured 17-4 stainless steel, Materials and Design,133 (2017) 205–215.

[5] L. Facchini, N. Vicente Jr., I. Lonardelli, E. Magalini, P. Robotti, A. Molinari, Metastable austenite in 17-4 Precipitation-Hardening stainless steel produced by Selective Laser Melting of powders and its effect on tensile properties, Advanced Engineering Materials,12-3 (2010) 184-188.

[6] Y. Sun, R.J. Hebert, M.Aindow, Effect of heat treatments on microstructural evolution of additively manufactured and wrought 17-4 PH stainless steel, Materials and Design, 156 (2018) 429-440.

[7] T. L. Starr, K. Rafi, B.Stucker, C. M. Scherzer, Controlling phase composition in selective laser melted stainless steels, Proceedings of Solid Freeform Fabrication Symposium (2012) 439–456.

[8] H.K. Rafi, D. Pal, N. Patil, T.L. Starr, B.E. Stucker, Microstructure and mechanical behavior of 17-4 precipitation hardenable steel processed by selective laser melting, Journal of Materials Engineering and Performance,23-12 (2014) 4421–4428.

[9] S.D. Meredith, J.S. Zuback, J.S. Keista, T.A. Palmer, Impact of composition on the heat treatment response of additively manufactured 17–4 PH grade stainless steel, Materials Science & Engineering A, 738 (2018) 44–56.

[10]H. K. Yeddu, Phase-field modeling of austenite grain size effect on martensitic transformation in stainless steels, Computational Materials Science, 154 (2018) 75-83.

[11] Y. Sun, R. J. Hebert, M. Aidow, Non-metallic inclusions in 17-4PH stainless steel parts produced by selective laser melting, Materials and Design, 140 (2018) 153–162.

[12] T. Mukherjee, J. S. Zuback, A. De, T. DebRoy, Printability of alloys for additive manufacturing, Scientifics Reports, 6:1-6 (2016) Article 19717.

[13] A. Kudzal, B. McWilliams, C. Hofmeister, F. Kellogg, J Yuc, J. Taggart-Scarff, J. Liang, Effect of scan pattern on the microstructure and mechanical properties of Powder Bed Fusion additive manufactured 17-4 stainless steel, Materials and Design, 133 (2017) 205–215.

[14] L. Thijs, F. Verhaeghe, T. Craeghs, J. Van Humbeeck, J.P. Kruth, A study of the micro structural evolution during selective laser melting of Ti-6Al-4V. Acta Materialia, 58-9 (2010) 3303–3312.

[15] T. DebRoy, H.L. Wei, J.S. Zuback, T. Mukherjee, J.W. Elmer, J.O. Milewski, A.M. Beese, A. Wilson-Heid, A. De, W. Zhang, Additive manufacturing of metallic components – Process, structure and properties, Progress in Materials Science, 92 (2018) 112–224.

\